Analysis of Frequency-Dependent Line-of-Sight Probability in 3-D Environment

Xiang Liu, Jing Xu, and Hongying Tang

***Abstract*— Since mmWave signals are sensitive to blockages, prior channel models including the LoS probability function for ultra-high frequency band cannot be applied directly to analyze mmWave cellular networks. Compared with the empirical LoS probability model obtained from the computationally intensive simulations and measurements, the theoretical LoS probability model in mmWave cellular networks still remains unclear. According to the Huygens-Fresnel principle for the wave propagation, the LoS probability is closely related to the carrier frequency. In this letter, the 3-D frequency-dependent LoS probability model incorporated with the Fresnel zone is presented, and shows good agreement with the empirical models adopted in the 3GPP standard for various scenarios.**

***Index Terms*— LoS probability, frequency-dependent, Fresnel zone.**

I. Introduction

PROPAGATION characteristics of the mmWave are being investigated because of its prospects in next generation communication systems [1]. Due to the higher penetration and diffraction losses for the mmWave [2], the performance of mmWave systems is mainly decided by the line-of-sight (LoS) transmission links [3], [4].

Basically, there are three methods for the channel modeling, i.e., empirical, deterministic and stochastic method [5]. For the empirical method, the LoS probability are obtained based on the curve fitting method for the real-world measurement data [1], [6]. This model is simple and efficient to use, but cannot be extended to the other environments with different characteristics. The deterministic model [7], [8] is derived from the electromagnetic-wave equation, and can provide a higher level of accuracy for the signal propagation prediction. However, a prior knowledge of the terrain information, such as the positions and sizes of obstructions, are required for the deterministic methods, which is unrealistic for most scenarios. The stochastic method explicitly models the environment settings as a series of random variables [5], and derives the analytical expression of the channel model [9]. The stochastic method provides acceptable estimations of the channel model with lower complexity, and has widely been used [9], [10].

Based on the stochastic method, Bai *et al.* [9] derived the theoretical LoS probability in 2D plane, where random buildings are modeled as a process of rectangles with random sizes and orientations whose centers form a Poisson Point Process on the plane. Therein, the LoS probability is treated as the visual LoS probability which is independent of the carrier frequency, that is the probability of no blockages intersecting with the visual sight line between the transmitter (TX) and receiver (RX), which is not accurate from the radio frequency propagation perspective [7], [11]. More specifically, extra space known as the Fresnel zone is needed for the radio frequency (RF) waves to communicate between two RF devices. Note that the Fresnel ellipsoid diameter is frequency-dependent, and has been used to obtain the LoS probability via deterministic model [7]. To the best of our knowledge, existing works neither derive the stochastic frequency-dependent LoS probability, nor exploit the 3D environment information.

In this letter, we extend the results in [9] to a more general 3D environment, and focus on the frequency-dependent LoS probability. The main contributions of our work are as follows:

- We propose a stochastic method to evaluate the frequency-dependent LoS probability in 3D environment, where the existence of LoS component is detected over *LoS Clearance zone*.
- Based on our model, we derive the analytical expression of LoS probability. It would be the first work in the literature that theoretically presents a joint impact on LoS probability by the height difference and distance between TX and RX, density of the obstruction buildings, as well as the carrier frequency.
- Numerical results show that our results match well with the models used in the 3GPP standards [12].

The letter is organized as follows. Section II briefly introduces the system model and problem formulation. The frequency-dependent LoS probability is analyzed in Section III. Numerical results for the frequency-dependent LoS probability and comparison with the visual LoS probability are provided in Section IV. Conclusions are drawn in Section V.

II. System Model and Problem Formulation

A. LoS Transmission

The radio frequency LoS transmission link is formed by all possible paths within the first Fresnel zone [11]. Denote the minimum ratio of the clearance for the first Fresnel zone as η [11]. The LoS Clearance Zone is defined as the elliptical area inside η of the first Fresnel zone as shown in Fig. 1, whose diameter equals to η of the first Fresnel ellipsoid diameter.

Manuscript received March 19, 2018; revised May 21, 2018; accepted May 23, 2018. Date of publication June 1, 2018; date of current version August 10, 2018. This work was supported by National Natural Science Foundation of China (Grant No. 61571303), the Inter-Government Key Program for International Scientific and Technological Innovation Cooperation Project of China (Grant No. 2016YFE0122900) and the Shanghai Municipal Natual Science Foundation (Grant No. 18ZR1437600). The associate editor coordinating the review of this letter and approving it for publication was D. Cassioli. *(Corresponding author: Jing Xu).*

X. Liu and J. Xu are with the Key Laboratory of Wireless Sensor Network & Communication, Shanghai Institute of Microsystem and Information Technology, Chinese Academy of Sciences, Shanghai 200050, China, and also with the University of Chinese Academy of Sciences, Beijing 100049, China (e-mail: xiang.liu@wico.sh; jing.xu@wico.sh).

H. Tang is with the Science and Technology on Micro-System Laboratory, SIMIT, Chinese Academy of Sciences, Shanghai 200050, China (e-mail: tanghy@mail.sim.ac.cn).

Digital Object Identifier 10.1109/LCOMM.2018.2842763

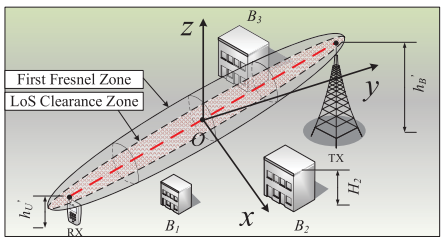

Fig. 1. The first Fresnel zone and LoS clearance zone.

For the LoS transmission of two RF devices, all possible paths within the LoS Clearance Zone should not be blocked.

As illustrated in Fig. 1, the locations of the TX and RX in 3D environment are described in the Cartesian coordinate system, where the midpoint of the line segment connecting the TX and RX is set as the original point. Then the xOy plane is parallel to the horizontal surface, and the vertical direction is set as z axis. The projection direction of the RX oriented to TX in the xOy plane is set as the y axis. Denote the height of TX and RX as h'_B and h'_U, respectively. Denote 3D distance between TX and RX as $r = \sqrt{d^2 + h_B^2}$, where d is the projection of r in the xOy plane, and $h_B = h'_B - h'_U$ is the height difference between TX and RX. The point (x, y, z) in the LoS Clearance Zone as depicted in Fig. 1 can be expressed as the anti-clockwise rotation of $\frac{x^2}{b^2} + \frac{y^2}{a_0^2} + \frac{z^2}{b^2} \leqslant 1$ about the x axis, the rotation angle is $\varphi\left(0 \leqslant \varphi \leqslant \frac{\pi}{2}\right)$, and $\cos\varphi = \frac{d}{r}$.

$$\frac{x^2}{b^2} + \frac{\left(y\cos\varphi - z\sin\varphi\right)^2}{a_0^2} + \frac{\left(y\sin\varphi + z\cos\varphi\right)^2}{b^2} \leqslant 1, \quad (1)$$

where

$$\begin{cases} a_0 = \frac{r}{2} + \frac{\lambda}{4} \\ b = \eta\sqrt{\frac{r\lambda}{4} + \frac{\lambda^2}{16}}. \end{cases} \quad (2)$$

Note that $\lambda \to 0$ results in $a_0 = r/2, b = 0$, then the LoS Clearance Zone reduces to the direct line connecting TX and RX, which corresponds to the 3D visual LoS case.

B. Problem Formulation

We adopt the similar assumptions as [9] in 2D plane: the obstructions of the system are assumed to be the cuboid buildings $\{B_k\}$, whose locations in xOy plane are modeled to be the homogenous Poisson Point Process (HPPP) Φ with intensity λ_B; the locations of buildings $\{B_k\}$ in the xOy plane are denoted as $\{C_k\}$, then $\{C_k\} \in \Phi$; the length L_k and width W_k of building B_k are independent from each other and are assumed to be independent identically distributed (i.i.d.) according to probability density function (PDF) $f_L(l)$ and $f_W(w)$, respectively. The direction Θ_k of B_k is uniformly distributed in $(0, 2\pi]$. In addition, the height H_k of building B_k is uniformly distributed in $(h'_L, h'_H]$ for the 3D environment. The PDF of H_k and Θ_k are denoted as $f_H(h)$ and $f_\Theta(\theta)$, respectively. Let $h_H = h'_H - h'_U$ and $h_L = h'_L - h'_U$.

Denote Ω and Π_k as the LoS Clearance Zone and the cuboid area of building B_k, respectively. According to the definition of the LoS transmission [11], the LoS transmission requires that area Π_k should not intersect with Ω. Hence, the frequency-dependent LoS probability equals to the probability that the union for the intersection of Ω and Π_k is an empty set, i.e.,

$$P_{LoS} = P\left(\bigcup_{k, C_k \in \Phi} \left\{\Omega \bigcap \Pi_k\right\} = \varnothing\right). \quad (3)$$

Define the indicator function as

$$\mathbf{1}_\Omega\left(\Pi_k\right) = \begin{cases} 0, & \Omega \bigcap \Pi_k = \varnothing \\ 1, & \Omega \bigcap \Pi_k \neq \varnothing, \end{cases} \quad (4)$$

then the number of the buildings that obstruct into the LoS Clearance Zone is expressed as

$$N = \sum_{k, C_k \in \Phi} \mathbf{1}_\Omega\left(\Pi_k\right). \quad (5)$$

Hence, the frequency-dependent LoS probability equals to the probability of $N = 0$, or i.e., $P_{LoS} = P\left(N = 0\right)$.

III. Frequency-Dependent LoS Probability

A. Frequency-Dependent LoS Probability

The point process formed by the locations $\{C_k^{l,w,h,\theta}\}$ of the centers of the buildings with the same parameter $(W_k = w, L_k = l, H_k = h, \Theta_k = \theta) \in (w + dw, l + dl, h + dh, \theta + d\theta)$ is denoted as $\Phi_{w,l,h,\theta}$. According to the independent thinning process [13] of the Poisson Point Process, $\Phi_{w,l,h,\theta}$ is a PPP with the density $\lambda_{w,l,h,\theta}$, which is calculated as

$$\lambda_{w,l,h,\theta} = \lambda_B f_W(w)\, dw f_L(l)\, dl f_H(h)\, dh f_\Theta(\theta)\, d\theta. \quad (6)$$

Moreover, due to the independency between W_k, L_k, H_k and Θ_k, if $(w_1, l_1, h_1, \theta_1) \neq (w_2, l_2, h_2, \theta_2)$, $\Phi_{w_1,l_1,h_1,\theta_1}$ and $\Phi_{w_2,l_2,h_2,\theta_2}$ are independent from each other.

Let $N_{w,l,h,\theta}$ be the number of the buildings that obstruct into the LoS Clearance Zone with parameter (w, l, h, θ),

$$N_{w,l,h,\theta} = \sum_{k, C_k \in \Phi_{w,l,h,\theta}} \mathbf{1}_\Omega\left(\Pi_k\right), \quad (7)$$

then the total number N can be rewritten as

$$N = \sum_{w,l,h,\theta} N_{w,l,h,\theta}. \quad (8)$$

Since $\Phi_{w,l,h,\theta}$ and Φ are both PPP, $N_{w,l,h,\theta}$ and N are both Poisson distributed random variables. The frequency-dependent LoS probability is expressed as

$$P_{LoS}\left(d, h_B, \lambda_B, \lambda\right) = P\left(N = 0\right) = \exp\left(-\mathbb{E}\left[N\right]\right). \quad (9)$$

From equation (9), one can see that the LoS probability depends on the expected value of N. As the first step, we give the following lemma.

Lemma 1: The expected value of $N_{w,l,h,\theta}$ is calculated as

$$\mathbb{E}\left[N_{w,l,h,\theta}\right] = \lambda_{w,l,h,\theta} \begin{bmatrix} 2w\sqrt{b^2\sin^2\theta + c_2^2\cos^2\theta} \\ +2l\sqrt{b_1^2\cos^2\theta + c_1^2\sin^2\theta} \\ +wl + A_1 + A_2 \end{bmatrix},$$

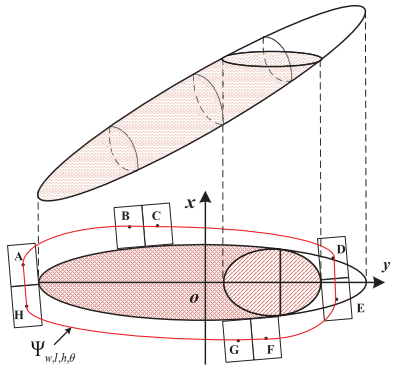

Fig. 2. The shadowing region in the xOy plane is the projection of the LoS clearance zone. Any rectangle will intersect with the LoS clearance zone if and only if its center falls into the region $\Psi_{w,l,h,\theta}$ surrounded by the centers of the buildings which are tangent to the LoS clearance zone.

where

$$\begin{cases} b_1^2 = b^2 - \dfrac{b^2h^2}{b^2\cos^2\varphi + a_0^2\sin^2\varphi}, \\ c_1^2 = \dfrac{b^4a_0^2\cos^2\varphi + b^2a_0^4\sin^2\varphi - b^2a_0^2h^2}{\left(b^2\cos^2\varphi + a_0^2\sin^2\varphi\right)^2}, \\ c_2^2 = b^2\sin^2\varphi + a_0^2\cos^2\varphi, \\ A_1 = \dfrac{b_1c_1}{2}\left(\pi - \sin\left(2\arcsin\dfrac{y_0 - r_1}{c_1}\right) - 2\arcsin\dfrac{y_0 - r_1}{c_1}\right), \\ A_2 = \dfrac{bc_2}{2}\left(\pi + \sin\left(2\arcsin\dfrac{y_0}{c_1}\right) + 2\arcsin\dfrac{y_0}{c_1}\right), \\ y_0 = \dfrac{\left(b^2\sin^2\varphi + a_0^2\cos^2\varphi\right)h}{\left(a_0^2 - b^2\right)\sin\varphi\cos\varphi}. \end{cases}$$

Proof: As shown in Fig. 2, the points $A, B, ..., G$ represent the centers of the buildings from $\Phi_{w,l,h,\theta}$ in the xOy plane. The corresponding rectangles are tangent to the projection of LoS Clearance Zone. Let $\Psi_{w,l,h,\theta}$ represents the region surrounded by the centers of the buildings which are tangent to the projection of the LoS Clearance Zone. Then the cuboid building from $\Phi_{w,l,h,\theta}$ obstructs into the LoS Clearance Zone if and only if its center falls into the region $\Psi_{w,l,h,\theta}$ depicted in Fig. 2. Since $N_{w,l,h,\theta}$ is a Poisson distributed random variable, its expected number is calculated as $\mathbb{E}\left(N_{w,l,h\theta}\right) = \lambda_{w,l,h,\theta}S_{\Psi_{w,l,h,\theta}}$, where $S_{\Psi_{w,l,h,\theta}}$ represents the area of $\Psi_{w,l,h,\theta}$ and can be calculated as

$$\begin{aligned} S_{\Psi_{w,l,h,\theta}} &= 2w\sqrt{b^2\sin^2\theta + c_2^2\cos^2\theta} \\ &\quad + 2l\sqrt{b_1^2\cos^2\theta + c_1^2\sin^2\theta} + wl + A_1 + A_2. \end{aligned} \tag{10}$$

Based on the analytic geometry theory, $S_{\Psi_{w,l,h,\theta}}$ can be easily derived as shown in (10). ∎

According to (8), and based on Lemma 1, the expected value of N can be calculated as the sum for $N_{w,l,h,\theta}$

$$\begin{aligned} \mathbb{E}\left[N\right] &= \mathbb{E}\left[\sum_{w,l,h,\theta} N_{w,l,h,\theta}\right] = \sum_{w,l,h,\theta}\mathbb{E}\left[N_{w,l,h,\theta}\right] \\ &= \int_{w,l,h,\theta} S_{\Psi_{w,l,h,\theta}}\lambda_B f_W(w)dw f_L(l)dl f_H(h)dh f_\Theta(\theta)d\theta \\ &= \int_h \lambda_B\left(d_1\left(\bar{W} + \bar{L}\right) + \bar{W}\bar{L} + A_1 + A_2\right) f_H(h)\,dh, \end{aligned} \tag{11}$$

where

$$\begin{cases} d_1 = \frac{2r_1}{\pi} + \frac{2c_1E\left(\sqrt{1-\frac{b_1^2}{c_1^2}}\right)}{\pi} + \frac{2c_2E\left(\sqrt{1-\frac{b_2^2}{c_2^2}}\right)}{\pi}, \\ r_1 = h\frac{\left(a_0^2 - b^2\right)\sin\varphi\cos\varphi}{\left(b^2\cos^2\varphi + a_0^2\sin^2\varphi\right)}, \end{cases}$$

where $E(\cdot)$ represents the complete elliptic integral of the second kind, $\bar{W}$ and $\bar{L}$ represent the expected width and length of buildings, respectively. In the following subsection, we will discuss three special cases, where closed-form expressions of LoS probability can be obtained.

B. Closed-Form Expressions for Special Cases

In 2D frequency-dependent case, ignoring the height difference between TX and RX and height of buildings, then the LoS probability is expressed as

$$\begin{aligned} P_{LoS}^{2D}(d, \lambda_B, \lambda) &= P_{LoS}(d, h_B = 0, \lambda_B, \lambda) \\ &= \exp\left(-\lambda_B\left(\begin{array}{c}\frac{2\left(\bar{W}+\bar{L}\right)}{\pi}2a_0E\left(\sqrt{1-\frac{b^2}{a_0^2}}\right) \\ +\bar{W}\bar{L} + \pi a_0 b\end{array}\right)\right). \end{aligned} \tag{12}$$

In 2D visual LoS case, the LoS probability has been investigated in [9]. It can be calculated by further ignoring the impact of carrier frequency in (12), or i.e.,

$$\begin{aligned} P_{VLoS}^{2D}(d, \lambda_B) &= \lim_{\lambda\to 0} P_{LoS}(d, h_B = 0, \lambda_B, \lambda) \\ &= \exp\left(-\lambda_B\left(\frac{2\left(\bar{W}+\bar{L}\right)}{\pi}d + \bar{W}\bar{L}\right)\right). \end{aligned} \tag{13}$$

2D visual LoS probability as shown in (13) is exactly the same as the result in [9], which indicates the accuracy of the proposed method.

The visual LoS probability in this case is larger than the 2D frequency-dependent LoS probability in (12), due to the smaller LoS Clearance Zone with $a_0 = d/2$ and $b = 0$.

In 3D visual case, the LoS probability can be calculated by letting $\lambda \to 0$,

$$\begin{aligned} &P_{VLoS}^{3D}(d, h_B, \lambda_B) \\ &\quad= \lim_{\lambda\to 0} P_{LoS}(d, h_B, \lambda_B, \lambda) \\ &\quad= \exp\left(-\lambda_B\left(\frac{\left(\bar{W}+\bar{L}\right)(h_H + h_L)}{\pi h_B}d + \bar{W}\bar{L}\right)\right). \end{aligned} \tag{14}$$

From (14), one can see that, the LoS probability exponentially decays with the distance between TX and RX. Although it is obtained in 3D visual case, the same trend will also be observed in general numerical results, as shown in the next section.

IV. Numerical Results

Numerical results of the LoS probability are illustrated in this section. The expected width and length of the building are $\mathbb{E}(W)$=15m and $\mathbb{E}(L)$=15m, respectively. The density of the buildings is $\lambda_B = 0.1/\left(\mathbb{E}(W)\,\mathbb{E}(L)\right)$. The heights of TX and RX are $h_U' = 1.5$m and $h_B' = 35$m, respectively. The height bounds of buildings are h_L'=10m and h_H'=100m, respectively. The minimum clearance ratio of the Fresnel zone is $\eta = 0.6$.

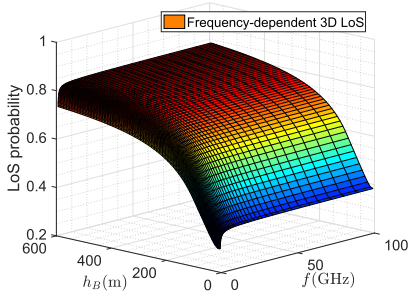

Fig. 3. The frequency-dependent 3D LoS probability versus the carrier frequency and height difference between TX and RX.

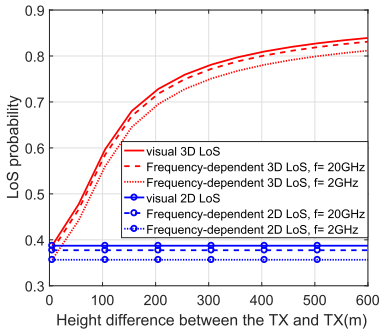

Fig. 4. The LoS probability versus the height difference between TX and RX.

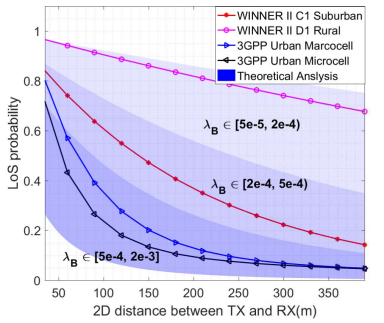

Fig. 5. The LoS probability versus the 2D distance between TX and RX.

The 3D frequency-dependent LoS probability versus the carrier frequency f and height difference between TX and RX h_B is depicted in Fig. 3. It can be seen that with the increase of f, the 3D frequency-dependent LoS probability given h_B asymptotically approaches a constant level. Another observation is that the LoS probability increases with frequencies and the height difference, matching the experimental trends observed in prior work [7].

The frequency-dependent LoS probability versus the height difference between TX and RX h_B in different cases are depicted in Fig. 4. It can be found that the frequency-dependent 2D and 3D LoS probability are upper bounded by the visual 2D and 3D LoS probability, respectively.

The LoS probability versus 2D distance between the RX and TX d are illustrated in Fig. 5. The measurement of LoS probability for the various kinds of environments [6] [12] falls into some regions determined by parameter λ_B, validating the accuracy of our channel model.

Note that for small d, the LoS probability obtained from the proposed results slightly deviates from that in the 3GPP standards for the Urban Marcocell. This can be explained by the fact the homogenous distribution of buildings λ_B is assumed for simplicity, which cannot adequately characterizes the statistics of the real-world environment. We leave a more practical model assumption of λ_B as a topic of future work.

V. Conclusion

In this letter, we proposed the stochastic method to evaluate the LoS probability from the radio frequency propagation perspective in 3D environment. Based on our method, we derived the analytical expression of the frequency-dependent LoS probability, exploiting its dependence with the distance between TX and RX. Numerical results indicate that the frequency-dependent LoS probability asymptotically approaches the visual LoS probability with the increase of the carrier frequency. Furthermore, our stochastic channel model shows good agreement with the empirical models adopted in the 3GPP standard for various scenarios.

References

[1] M. R. Akdeniz *et al.*, "Millimeter wave channel modeling and cellular capacity evaluation," *IEEE J. Sel. Areas Commun.*, vol. 32, no. 6, pp. 1164–1179, Jun. 2014.

[2] T. S. Rappaport *et al.*, "Millimeter wave mobile communications for 5G cellular: It will work!" *IEEE Access*, vol. 1, pp. 335–349, May 2013.

[3] A. K. Gupta, J. G. Andrews, and R. W. Heath, "Macrodiversity in cellular networks with random blockages," *IEEE Trans. Wireless Commun.*, vol. 17, no. 2, pp. 996–1010, Feb. 2018.

[4] K. Venugopal and R. W. Heath, "Millimeter wave networked wearables in dense indoor environments," *IEEE Access*, vol. 4, pp. 1205–1221, Mar. 2016.

[5] V. S. Abhayawardhana, I. J. Wassell, D. Crosby, M. P. Sellars, and M. G. Brown, "Comparison of empirical propagation path loss models for fixed wireless access systems," in *Proc. IEEE 61st Veh. Technol. Conf.*, May/Jun. 2005, pp. 73–77.

[6] J. Meinilä, P. Kyösti, T. Jämsä, and L. Hentilä, *WINNER II Channel Models*. Hoboken, NJ, USA: Wiley, 2009.

[7] J. Jërveläinen, S. L. H. Nguyen, K. Haneda, R. Naderpour, and U. T. Virk, "Evaluation of millimeter-wave line-of-sight probability with point cloud data," *IEEE Wireless Commun. Lett.*, vol. 5, no. 3, pp. 228–231, Jun. 2016.

[8] J.-H. Lee, J.-S. Choi, and S.-C. Kim, "Cell coverage analysis of 28 GHz millimeter wave in urban microcell environment using 3-D ray tracing," *IEEE Trans. Antennas Propag.*, vol. 66, no. 3, pp. 1479–1487, Mar. 2018.

[9] T. Bai, R. Vaze, and R. W. Heath, Jr., "Analysis of blockage effects on urban cellular networks," *IEEE Trans. Wireless Commun.*, vol. 13, no. 9, pp. 5070–5083, Sep. 2014.

[10] T. Ding, M. Ding, G. Mao, Z. Lin, D. López-Pérez, and A. Y. Zomaya, "Uplink performance analysis of dense cellular networks with LoS and NLoS transmissions," *IEEE Trans. Wireless Commun.*, vol. 16, no. 4, pp. 2601–2613, Apr. 2017.

[11] D. D. Coleman and D. A. Westcott, *CWNA: Certified Wireless Network Administrator Official Study Guide: Exam PW0-105*, 3rd ed. Alameda, CA, USA: SYBEX, 2012.

[12] *3rd Generation Partnership Project; Technical Specification Group Radio Access Network; Study On 3D Channel Model for LTE (Release 12)*, document 3GPP TR 36.873, 2014.

[13] D. Stoyan, W. S. Kendall, and J. Mecke, *Stochastic Geometry and Its Applications* (Wiley Paperback Series), 2nd ed. Hoboken, NJ, USA: Wiley, 2008.